Journal of Peptide Science, Vol. 3, 336–346 (1997)

Conformation of Four Peptides Corresponding to the α-Helical Segments of Human GM–CSF

STELLA FIORI[1], STEFANO MAMMI[1], EVARISTO PEGGION[1], PAOLO ROVERO[2], STEFANO PEGORARO[2] and ROBERTO P. REVOLTELLA[2]

[1]University of Padova, Department of Organic Chemistry, CNR, Biopolymer Research Center, Padova, Italy
[2]CNR, Institute of Mutagenesis and Differentiation, Pisa, Italy

Received 15 October 1996
Accepted 12 December 1996

Abstract: The conformation of segments corresponding to the four α-helical stretches found in human granulocyte-macrophage colony-stimulating factor was studied in water solution in the presence of different amounts of 2,2,2-trifluoroethanol (TFE). The CD spectra reveal the onset of secondary structure upon addition of TFE. The final amount of helical conformation varies among the four peptides. In all cases, the conformational transition is complete before 50% TFE (v/v). ^{1}H-NMR studies were conducted at this solvent composition, leading to the assignment of all the resonances and to the definition of the secondary structure for all four fragments. © 1997 European Peptide Society and John Wiley & Sons, Ltd.

J. Pep. Sci. 3: 336–346

No. of Figures: 12. No. of Tables: 5. No. of References: 25

Keywords: hGM-CSF segments; conformation; CD and NMR studies

INTRODUCTION

The differentiation, proliferation and maturation of the various haematopoietic cells and cell precursors are effected by a family of glycoproteins which includes colony-stimulating factors (CSFs) and interleukins (ILs). One of the first member of this family to be isolated was the granulocyte and macrophage colony-stimulating factor (GM–CSF) [1]. This glycoprotein causes the proliferation and differentiation of several components of the haematopoietic tree, i.e. granulocytes, macrophages, but also eosinophils and megakaryocytes [2, 3] Clinical uses of GM–CSF have been proposed for treatment of all pathologies requiring an increase of aspecific immunological response, including myelodysplastic syndromes [4], acquired immunodeficiency syndrome [5, 6], chemotherapy-induced myelosuppression and autologous bone marrow transplantation [7].

Mature human GM–CSF is a 127 residue protein obtained from a 144 residue precursor. It is glycosylated at Asn^{27} and Asn^{37} to give a total molecular weight between 18 and 22 kDa and contains two disulphide bridges, one between Cys^{54} and Cys^{96} and the other between Cys^{88} and Cys^{121}. The crystal

Abbreviations: CD, circular dichroism; DQF-COSY, double quantum filter correlation spectroscopy; ES-MS, electrospray-mass spectrometry; HBTU, [2-(1H-benzotriazolyl)-*N*,*N*,*N*′*N*′-tetramethyluronium hexafluorophosphate; hGm–CSF, human granulocyte-macrophage colony-stimulating factor; NMP, N-methylpyrrolidone NOESY, (two-dimensional ^{1}H) nuclear Overhauser enhancement spectroscopy; TFE, 2,2,2-trifluoroethanol; TOCSY, (two-dimensional ^{1}H) total correlation spectroscopy; Trt, trityl.

Address for correspondence: Prof. Evaristo Peggion, Department of Organic Chemistry, University of Padova, Via Marzolo 1, 35131 Padova, Italy

CCC 1075-2617/97/050336-11 $17.50

Table 1 Sequences and Analytical Characterization of the Peptides Studied in this Work

Helix[a]	Abbreviation	Sequence	MW[b]	Yield[c] (%)	Purity[d] (%)	R_t[e] (%)
A	GM–CSF(14–28)	Ac-EHVNAIQEARRLLNL-NH_2	1817	89	76	13.3
B	GM–CSF(55–65)	Ac-LQTRLELYKQG-NH_2	1389	95	86	10.2
C	GM–CSF(73–87)	Ac-LKGPLTMMASHYKQH-NH_2	1783	60	71	11.5
D	GM–CSF(102–115)	Ac-TFESFKENLKDFLL-NH_2	1772	79	82	14.7

[a]Position of the helix in the tertiary folding of GM-CSF. [b]Molecular weight determined by FAB mass spectrometry. [c]Yield of the crude product, referred to the resin loading. [d]HPLC purity of the crude product. [e]HPLC retention time (min); see Materials and Methods for chromatographic conditions.

structure of recombinant hGM–CSF has been recently solved by two groups independently [8, 9]; the global fold is similar to that of many other factors of this family [10], the main feature being a left-handed four α-helix bundle. Helix A comprises residues 13–28, helix B residues 55–64, helix C residues 74–87, and helix D residues 103–116 [8]. The structure of recombinant hGM–CSF also comprises two short β-strands.

The receptor for GM–CSF is a protein made of an α and a β chain whose primary sequences are known [11, 12]. The α chain alone is able to bind GM–CSF with low affinity. The β chain does not bind GM–CSF by itself, but the affinity of the entire receptor is almost three orders of magnitude higher than that of the isolated α chain. From structure–activity relationship studies the hypothesis has been made that the α chain of the receptor interacts with helix D and the C-terminal portion of helix A, while the β chain interacts with helix C and the N-terminal portion of helix A [13].

The scope of our work is to determine the shortest fragment of hGM–CSF still able to maintain the biological activities of the native protein. To this end we have prepared four peptides corresponding to the four α-helices (Table 1) and we have studied their conformational tendencies in solution. Although these peptides are not likely to be active as such, they constitute our building blocks to obtain more complicated constructs with the desired properties.

MATERIALS AND METHODS

Materials

The four peptides were synthesized by the solid-phase method using a Milligen 9050 automatic synthesizer with Fmoc/tBu chemistry and continuous flow technology. Each peptide was prepared on a 0.07 mmol scale, using 0.5 g of PAL–PEG-PS resin (substitution level: 0.14 mmol/g), characterized by a 5-(4-aminomethyl-3,5-dimethoxyphenoxy) valeric acid linker (PAL) on a polystyrene-supported polyoxyethylene scaffold (PEG-PS). The PAL linker is necessary in order to obtain C-terminal amides, while the PEG-PS support allows one to use a high-flow rapid protocol. The following side-chain protections were used: tBu for Asp, Glu, Tyr, Thr and Ser; Trt for Asn, Gln and His; Pmc for Arg, and Boc for Lys. Coupling reactions were carried out using a four-fold excess of protected amino acid, with HBTU/HOBT activation and the high-flow rapid protocol routinely used in our laboratory with PEG-PS resins, i.e. recycle through the resin for 15 min at a flow rate of 16.2 ml/min. Similarly, Fmoc deprotection was achieved with piperidine (20% in DMF) for 3.5 min at 8.1 ml/min. After the last coupling and deprotection, the N-terminal amino function was acetylated by treatment with acetic anhydride and DIEA in DMF. Cleavage from the resin and side-chain deprotection were achieved by treatment of the dried peptide–resin with 10 ml of a mixture of trifuoroacetic acid/anisole/ethanedithiol (95 : 2.5 : 2.5 v/v) for 1.5 h at room temperature. The crude peptides were precipitated with cold diethyl ether and lyophilized; the yields are reported in Table 1. In the case of peptide C the cleavage procedure was performed under N_2, because of the presence of two Met residues which are sensitive to air oxidation during acidic treatment; nevertheless, 15% of Met sulphoxide was detected in the crude mixture. The oxidized peptide was identified by comparison with a standard obtained by H_2O_2.

The crude peptides were analysed by HPLC on a Beckman System Gold apparatus in the following conditions: Vydac C_{18} column (0.46 × 15 cm^3); eluent A, 0.1% TFA in water; eluent B, 0.1 TFA in acetonitrile; gradient from 5% to 65% B over 20 min; flow, 1 ml/min; detection, UV, 210 nm. HPLC pu-

rities are reported in Table 1 (expressed as peak area %). The main peak (R_1 are reported in Table 1) was isolated by preparative HPLC, using a Vydac C_{18} column (2.2 × 25 cm^2); eluents A and B as indicated above; gradient from 15% to 30% B over 60 min; flow, 8 ml/min; detection, UV, 210 nm. The final products (HPLC purity >99%) yielded the correct amino acid ratios in the amino acid analysis of the acid hydrolysates, and the correct molecular weight as determined by FAB-MS (Table 1).

CD Experiments

Circular dichroism spectra were obtained on a Jasco Model J-600 A automatic recorder spectropolarimeter. All measurements were performed at room temperature in quartz cells of path lengths ranging from 0.001 to 0.1 cm. Spectra were obtained with a 2.0 nm bandwidth, time constants of 4 s and a scan speed of 10 nm/min; four to eight scans were co-added to improve the signal to noise ratio and the solvent baseline was recorded and subtracted from the spectra of the samples. All CD spectra were smoothed using the Jasco FT noise reduction software, and are reported in terms of ellipticity units per mole of peptide residue ($[\Theta]_R$). The helix content was estimated by the amplitude of the CD band at 220 nm according to Greenfield and Fasman [14]. The helix contents reported in a preliminary account of this work [15] were calculated using the method of Siegel *et al.* [16] and are higher than those reported here. pH measurements were performed with a Metrohm model 691 pH-meter calibrated with buffer solutions from Hanna Instruments.

NMR Experiments

NMR spectra were obtained on a Bruker AM 400 spectrometer. The data were processed on a Bruker X-32 workstation. Data were collected at 25 °C on 3 mM peptide solutions in H_2O/2,2,2-trifluoroethanol-d_3) (TFE-d_3) 1:1 (v/v), using tetramethylsilane as internal standard. The pH of the solutions was between 4 and 5 (uncorrected). The CD spectra of the solutions used for NMR experiments were identical to those of the 10^{-5} M solutions in the same solvent system. Two-dimensional homonuclear ^{1}H-NMR spectra were recorded in the pure absorption mode according to the TPPI method [17, 18] with 340–424 experiments of 2K data points. Prior to Fourier transformation the time domain data were multiplied by cosine squared or Gaussian window functions in both dimensions, and zero-filled to 2K × 1K real points. Fifth order polynomial baseline correction was performed in the ω_2 dimension after transformation.

In the acquisition of the DQF-COSY spectra [19], appropriate phase cycles were used to allow the suppression of rapid pulsing artefacts [20]. Two-dimensional homonuclear Hartmann-Hahn spectra were obtained as proposed by Griesinger *et al.* [21] (clean TOCSY). The MLEV-17 spin-lock sequence was applied with trim pulses of 2.5 ms each, using mixing times of 69–75 ms and spin-locking fields of 4.9–6.0 kHz. Two-dimensional NOESY spectra were recorded with the standard sequence [22] using 200 ms mixing times. The water signal was saturated by irradiation during the relaxation delay and, for NOESY spectra, also during the mixing time.

RESULTS

Circular Dichroism Measurements

The CD spectra of the four peptides in aqueous solution are typical of a random conformation with a negative maximum below 200 nm (Figures 1–5. A small amount of structural order (negative shoulder at about 220 nm) is observed in the case of sequences 14–28, 55–65 and 102–115. With the exception of sequence 14–28, the spectra are almost pH-independent in the range 3–10 and concentration-independent in the range 10^{-5}–10^{-3} M (data not shown). Quite differently, the sequence 14–28,

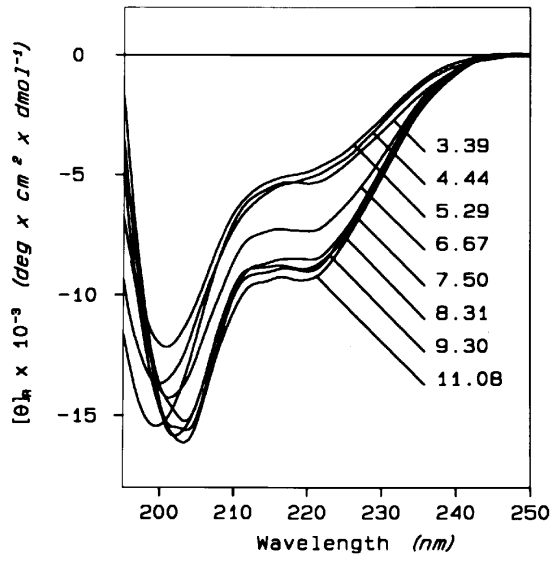

Figure 1 CD spectra of 4 × 10^{-5} M GM–CSF(14–28) in water at various pH values (indicated).

corresponding to helix A, shows an increase of molar ellipticity at 200 nm upon increasing the pH, indicating the partial onset of an α-helical structure (Figure 1). At 4×10^{-5} M, the conformational change occurs at about pH 6.5, in correspondence to the deprotonation of His[15]. The maximum helical content reaches about 30% around pH 9. If the experiment is repeated at 10^{-3} M peptide concentration, the conformational change is shifted between pH 5 and 6. This is an indication that the phenomenon of helix formation is accompanied by helix aggregation.

All peptides fold into the α-helical conformation in the presence of increasing amounts of TFE (Figures 2–5). In all cases, the spectra fit a well-defined isodichroic point indicating the presence of a two-component coil–helix equilibrium system. The titration curves relative to the four peptides are shown in Figure 6. The profile of the CD intensity at 220 nm vs. TFE content is S-shaped, indicating cooperativity of the solvent-induced conformational transition. The maximum helix content is reached at 25–35% TFE for all peptides but the percentage of helical structure differs significantly in the four segments. The helical contents at saturation conditions of the four segments, estimated according to Greenfield and Fasman [14], are the following: GM–CSF(14–28),

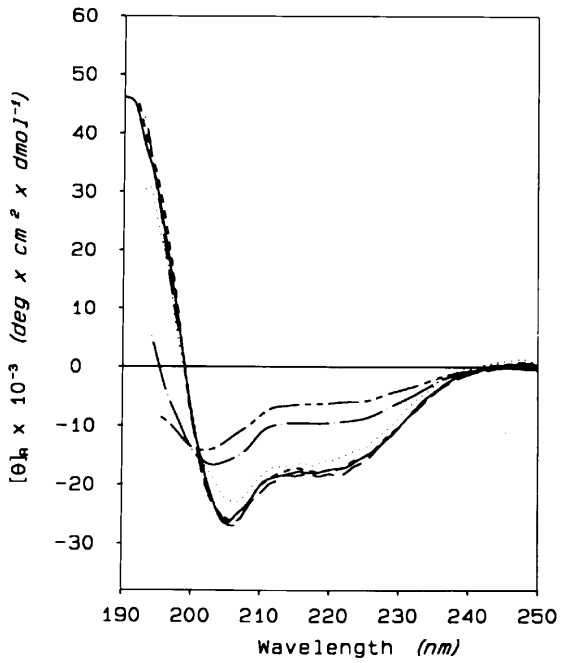

Figure 2 CD spectra of 4×10^{-5}M GM–CSF(14–28) in water/TFE at various percentages of TFE (v/v): – – – – 0%; – · – 10%; · · · · · 30%; - - - - 50%; - - - - - - - - 75%; —— 100%.

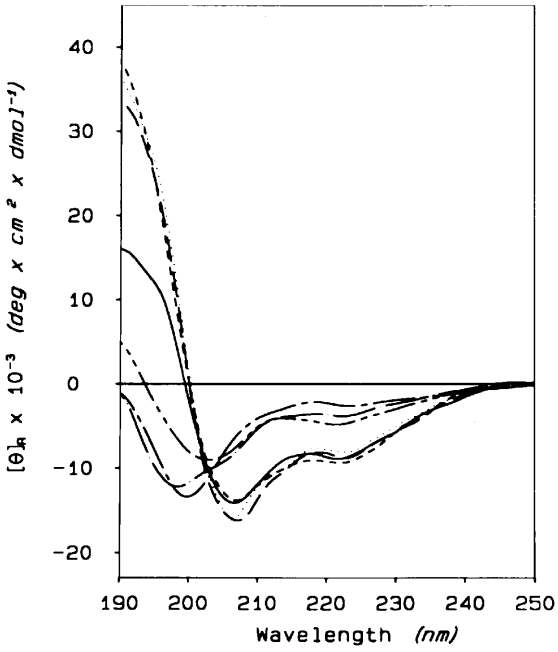

Figure 3 CD spectra of 2×10^{-5} M GM–CSF(55–65) in water/TFE at various percentages of TFE (v/v): – – – 0%, – · – 10%; – – – – 15%; —— 25%; - - - - 50%; – – – 75%; · · · · · 100%.

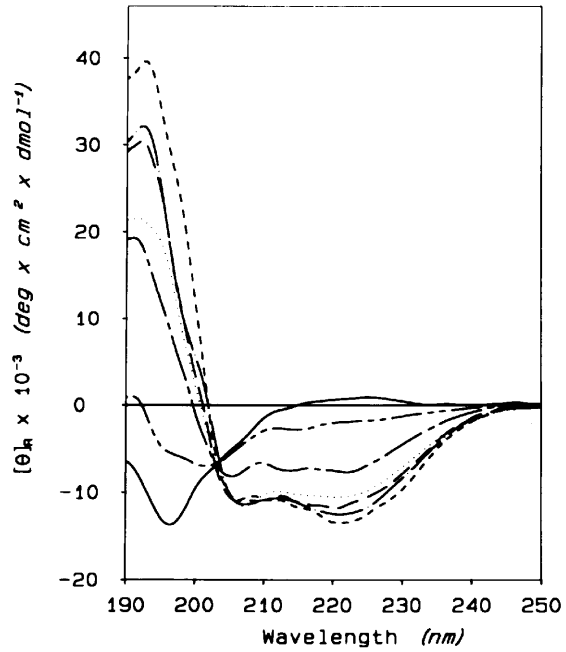

Figure 4 CD spectra of 2×10^{-5} M GM–CSF(73–87 in water/TFE at various percentages of TFE (v/v): —— 0%; – – – – 15%; – – – 25%; · · · · · 30%; – · – 50%; - - - - - - - - 75%; - - - - 100%.

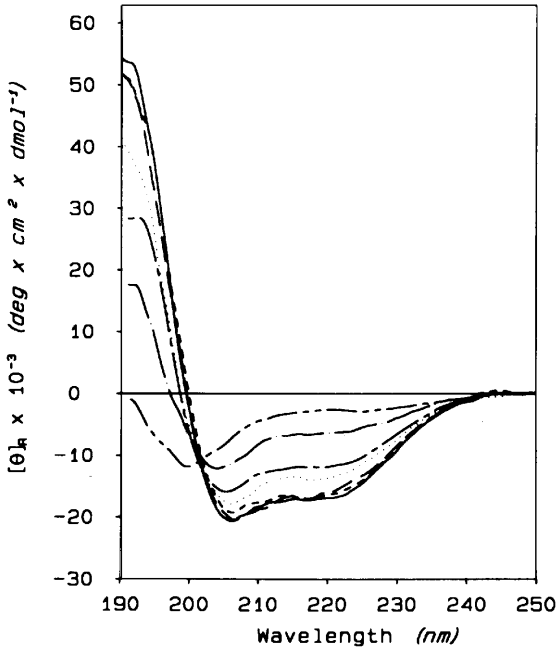

Figure 5 CD spectra of 3×10^{-5} M GM–CSF(102–115) in water/TFE at various percentages of TFE (v/v): – – – 0%; – · – 15%; – – – 20%; · · · · · 25%; —— 50%; - - - - 75%; ---------- 100%.

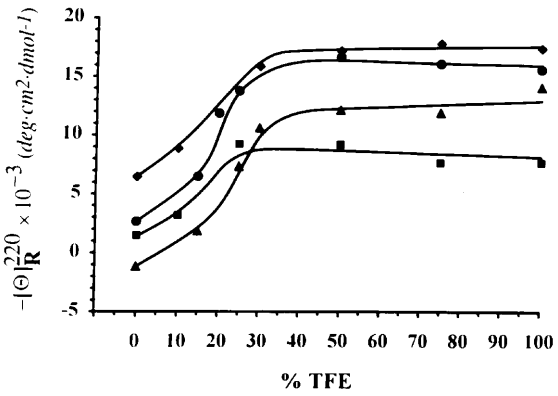

Figure 6 Plot of the molar ellipticity per residue as a function of percentage of TFE (v/v) for the four peptides: (◆) GM–CSF(14–28); (■) GM–CSF(55–65); (▲) GM–CSF(73–87); (●) GM–CSF(102–115).

56%; GM–CSF(55–65), 27%; GM–CSF(73–87), 39%; GM–CSF(102–115), 51%. Not surprisingly, the lowest amount of helix is observed with the shortest 11-residue sequence 55–65.

NMR Measurements

In light of the fact that in the 1:1 water/TFE mixture all peptides have adopted the maximum helical conformation, NMR studies were performed in this solvent system. The 3 mM solutions used in all NMR experiments exhibited the same CD spectra as the corresponding $\sim 10^{-5}$M solutions used in CD measurements, thus indicating that the conformational situations of the peptides in concentrated and dilute solutions are the same. Using standard two-dimensional experiments, the spin systems of all amino acid residues were identified and all the proton

Table 2 Proton Resonance Assignment of the Peptide GM–CSF(14–28) in 1:1 H_2O/TFE-d_3 Solution, $c = 3$ mM, $t = 298$ K, pH ~ 4.5

Residue	NH	C^{α}	$C^{\beta}H$	$C^{\gamma}H$	$C^{\delta}H$	Other protons
Ac						CH_3 2.10
Glu^{14}	8.14	4.31	1.99, 2.03	2.44, 2.47		
His^{15}	8.56	4.80	3.28, 3.39			H^4 7.34, H^2 8.64
Val^{14}	7.98	4.09	2.17	1.02, 1.04		
Asn^{17}	8.39	4.73	2.95			NH_2 7.61, 6.70
Ala^{18}	8.16	4.22	1.56			
Ile^{19}	7.76	3.89	2.03	1.30, 1.69	0.92	$C^{\gamma}H_3$ 0.99
Gln^{20}	8.08	4.09	2.27	2.46, 2.57		NH_2 7.17, 6.71
Glu^{21}	8.13	4.20	2.20, 2.23	2.54		
Ala^{22}	8.27	4.12	1.58			
Arg^{23}	8.23	4.02	2.00, 1.96	1.73	3.20, 3.24	$N^{\varepsilon}H$ 7.16
Arg^{24}	7.82	4.20	1.88, 2.07	1.74	3.28	$N^{\varepsilon}H$ 7.24
Leu^{25}	8.20	4.22	1.95, 1.65	1.65	0.94, 0.97	
Leu^{26}	8.13	4.29	1.87, 1.65	1.65	0.94	
Asn^{27}	7.86	4.67	2.87, 3.03			NH_2 7.58, 6.72
Leu^{28}	7.95	4.38	1.82, 1.68	1.82	0.95, 1.00	
NH_2	7.37, 6.87					

Table 3 Proton Resonance Assignment of the Peptide GM–CSF(55–65) in 1:1 H_2O/TFE-d_3 Solution, $C = 3$ mM, $T = 298$, pH ~ 4.5

Residue	NH	$C^{\alpha}H$	$C^{\beta}H$	$C^{\gamma}H$	$C^{\delta}H$	Other protons
Ac						CH_3 2.18
Leu^{55}	8.15	4.16	1.69	1.69	1.01, 0.96	
Gln^{55}	8.81	4.14	2.17	2.48		NH_2 7.36, 6.64
Thr^{57}	7.73	4.13	4.28	1.32		
Arg^{58}	7.83	4.13	1.99	1.78, 1.72	3.22	$N^{\varepsilon}H$ 7.16 NH_2 6.6
Leu^{59}	8.06	4.24	1.89, 1.66	1.86	0.98, 0.93	
Glu^{60}	8.02	4.17	2.28, 2.22	2.62, 2.56		
Leu^{61}	7.94	4.19	1.84, 1.57	1.81	0.94, 0.90	
Tyr^{62}	8.05	4.45	3.24, 3.19			Ar 7.18, 6.86
Lys^{63}	8.11	4.19	1.98	1.58	1.77	$C^{\varepsilon}H_2$ 3.06
Gln^{64}	8.09	4.33	2.29, 2.18	2.52		NH_2 6.90, 7.38
Gly^{65}	8.11	3.97				
NH_2	7.29, 6.71					

resonances of the four peptides were assigned. The proton chemical shifts are summarized in Tables 2–5. A few representative NOESY spectra are shown in Figures 7–9. The relevant NOESY connectivities found in the four peptides are reported in Figure 10. Finally, the deviations from the random coil position of the C^{α} proton resonances according to the method of Pastore and Saudek [23] are reported in Figure 11. Below, the conformational details of each peptide are discussed separately.

GM–CSF(14–28). Sequential and medium-range NOE cross-peaks suggest the presence of a helical structure that could include the whole peptide sequence, with the possible exception of the first two residues and of Lys^{10}. This conclusion is supported by the secondary shifts of C^{α} protons shown in Figure 11, with large negative deviations from N^{17} to L^{28}. According to these results, 12 out of 15 residues (80% of the sequence) are helical. This figure is definitely higher than that estimated from CD data (56%) and suggests fast exchange on the NMR timescale among conformers with different helical content. From the NMR data the two ends of the sequence seem to be more flexible than the central core.

Table 4 Proton Resonance Assignment of the Peptide GM–CSF(73–87) in 1:1 H_2O/TFE-d_3 Solution, $C = 3$ mM, $T = 298$, pH ~ 4.5

Residue	NH	$C^{\alpha}H$	$C^{\beta}H$	$C^{\gamma}H$	$C^{\delta}H$	Other protons
Ac						CH_3 2.10
Leu^{73}	7.78	4.36	1.67	1.73	0.96, 1.01	
Lys^{74}	7.92	4.34	1.88, 1.93	1.51	1.77	$C^{\varepsilon}H_2$ 3.04
Gly^{75}	8.32	4.03, 4.19				
Pro^{76}		4.38	2.05, 2.42	2.19	3.67, 3.87	
Leu^{77}	8.05	4.28	1.86, 1.69	1.81	0.97, 1.00	
Thr^{78}	7.97	4.06	4.41	1.35		
Met^{79}	8.11	4.33	2.27	2.61, 2.69		CH_3 2.11
Met^{80}	8.37	4.29	2.29, 2.32	2.65, 2.78		
Ala^{81}	8.56	4.23	1.59			
Ser^{82}	8.08	4.32	4.07			
His^{83}	8.01	4.62	3.31, 3.39			H^4 7.20, H^2 8.56
Tyr^{84}	8.12	4.51	3.15, 3.23			Ar 7.24, 6.91
Lys^{85}	8.03	4.27	1.90, 1.94	1.53	1.78	$C^{\varepsilon}H_2$ 3.07
Gln^{86}	8.06	4.29	2.09, 2.14	2.42, 2.45		NH_2 6.71, 7.41
His^{87}	8.23	4.69	3.23, 3.37			H^4 7.37, H^2 8.60
NH_2	7.50, 7.03					

Table 5 Proton Resonance Assignment of the Peptide GM–CSF(102–115) in 1:1 H_2O/TFE-d_3 Solution, $C = 3$ mM, $T = 298$, pH ~ 4.5

Residue	NH	$C^{\alpha}H$	$C^{\beta}H$	$C^{\gamma}H$	$C^{\delta H}$	Other protons
Ac						CH_3 2.14
Thr^{102}	7.87	4.33	4.33	1.25		
Phe^{103}	8.23	4.55	3.20			Ar 7.29
Glu^{104}	8.11	4.17	2.10	2.48		
Ser^{105}	8.04	4.29	3.95, 4.01			
Phe^{106}	8.00	4.43	3.23			Ar 7.23
Lys^{107}	8.03	3.92	1.86	1.41, 1.55	1.72	$C^{\epsilon}H_2$ 2.98
Glu^{108}	8.02	4.14	2.18	2.55		
Asn^{109}	8.02	4.60	2.81, 2.85			NH_2 7.33, 6.59
Leu^{110}	8.04	4.17	1.70, 1.56	1.67	0.89, 0.94	
Lys^{111}	7.99	3.97	1.94	1.47, 1.56	1.73	$C^{\epsilon}H_2$ 3.01
Asp^{112}	8.03	4.46	2.84, 2.97			
Phe^{113}	8.07	4.44	3.27			Ar 7.26
Leu^{114}	8.24	4.12	1.89, 1.54	1.93	0.94	
Leu^{115}	7.92	4.32	1.85, 1.64	1.83	0.91, 0.95	
NH_2	7.05, 6.79					

GM–CSF(55–65). This is the shortest peptide examined in the present study and very few medium-range connectivities were observed. The ones that are present (Figure 10B) are compatible with an α-helical structure in the sequence from Thr^{57} to Tyr^{62} (55% of the fragment), while the secondary shifts of C^{α} protons (Figure 11) seem to indicate an involvement of the entire sequence in this conformation. Thus, the helical content derived from NMR is at least twice that estimated from CD (55% vs. 27%). Again, rapid exchange among ordered and disordered conformers could be at the origin of this difference.

GM–CSF(73–87). The results obtained with this peptide are quite similar to those obtained with the first peptide. Intense medium-range connectivities

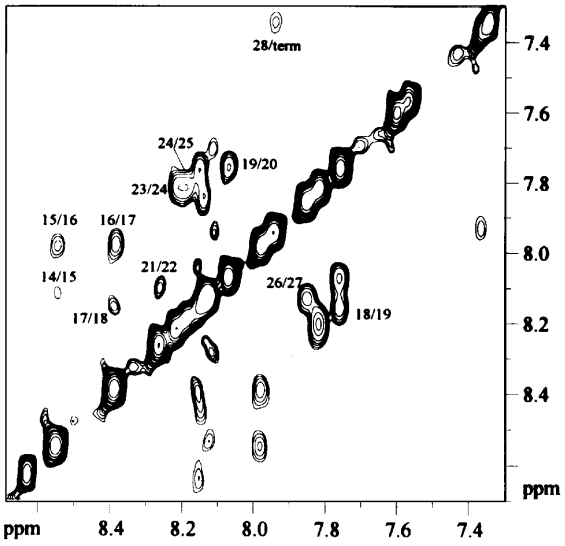

Figure 7 Amide region of a 200 ms NOESY spectrum of 3 mM GM–CSF(14–28) in H_2O/TFE-d_3 1:1. Sequential correlations are indicated.

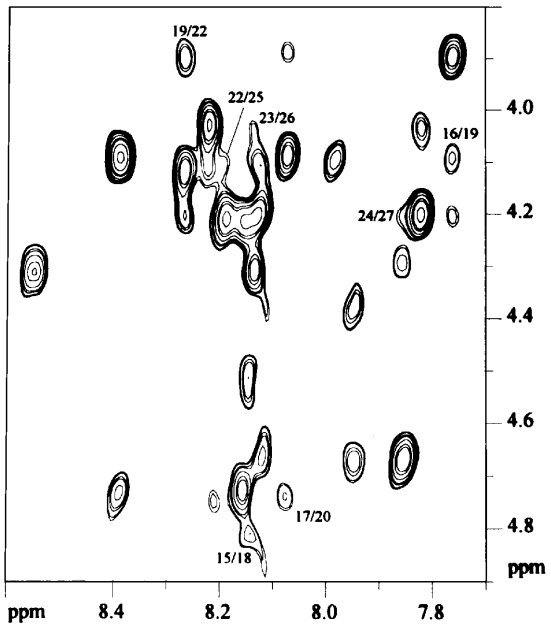

Figure 8 Fingerprint region of a 200 ms NOESY spectrum of 3 mM GM–CSF(14–28) in H_2O/TFE-d_3 1:1. Medium-range correlations are indicated.

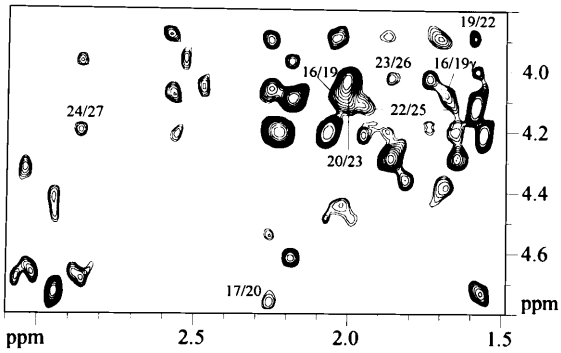

Figure 9 Fingerprint region of a 200 ms NOESY spectrum of 3 mM GM–CSF(14–28) in H_2O/TFE-d_3 1:1. Medium-range correlations are indicated.

are present starting from Pro^{76} where the helical stretch begins and makes up the rest of the sequence. The helical content based on these results and on the chemical shifts of the C^{α} protons is again much higher than that obtained by CD data (80% vs. 39%). For this result we offer the same explanation as for the previous cases, i.e. rapid exchange among conformers with different helical content.

GM–CSF(102–115). The medium-range connectivities found for this peptide span the entire sequence, indicating the involvement of all the residues in the formation of the helix. The secondary shifts of the C^{α} protons are in good agreement with these results, showing little difference among the various parts of the molecule. As for the peptides examined previously, the helical content is much higher than that obtained from CD (100% vs. 51%) and can be explained in the same way as for the previous cases.

DISCUSSION

The synthetic fragments corresponding to the four helices of GM–CSF tend to adopt, in TFE, the helical conformation found in the crystal structure of the native molecule [8]. The helix-forming propensity is

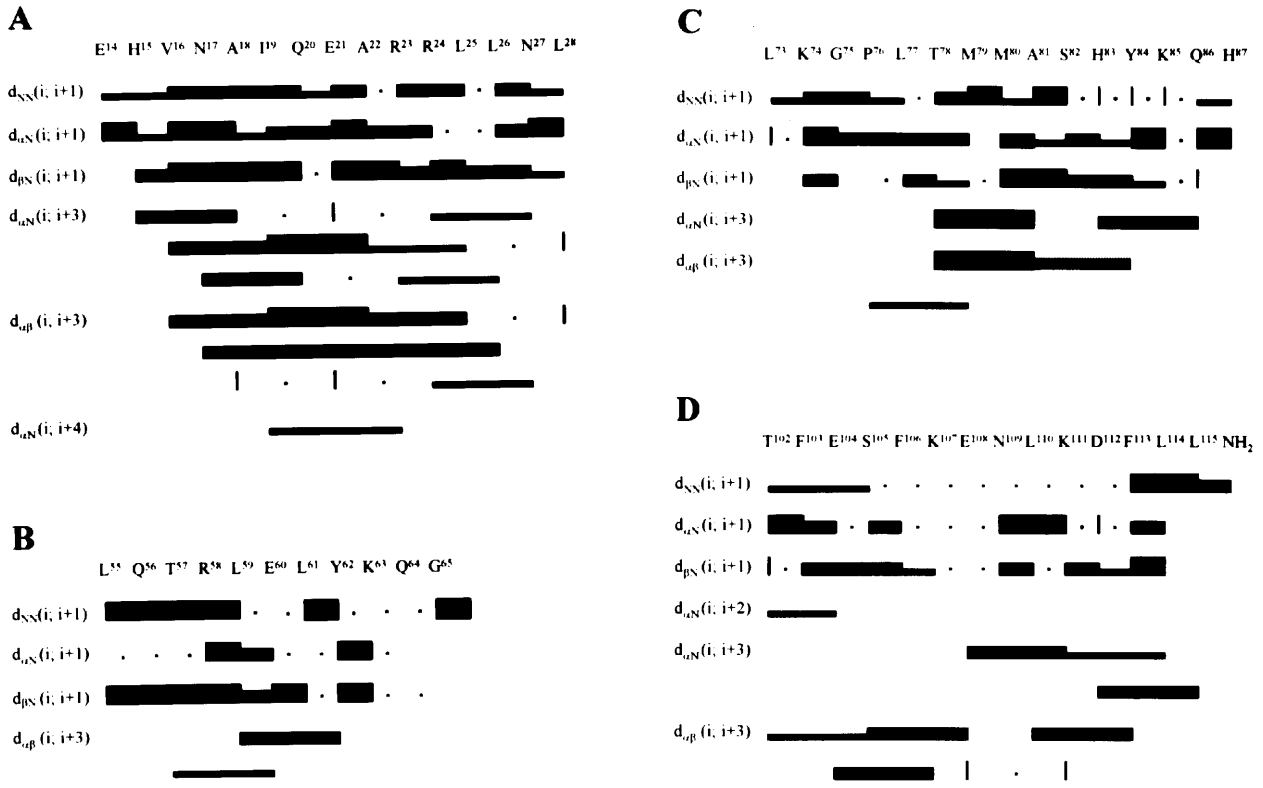

Figure 10 Summary of the NOESY correlations found for the four peptides in H_2O/d_3 1:1: (A), GM–CSF(14–28); (B), GM–CSF(55–65); (C), GM–CSF(73–87); (D) GM–CSF(102–115). The strength of NOEs, represented with bars of increasing thickness, is calculated from the volume of cross peaks in the NOESY spectra. Asterisks indicate effects between residues labelled by vertical bars, which were not measurable because of spectral overlap. The shaded area in panel C indicates a cross peak from a C^{α} proton to an aromatic side chain.

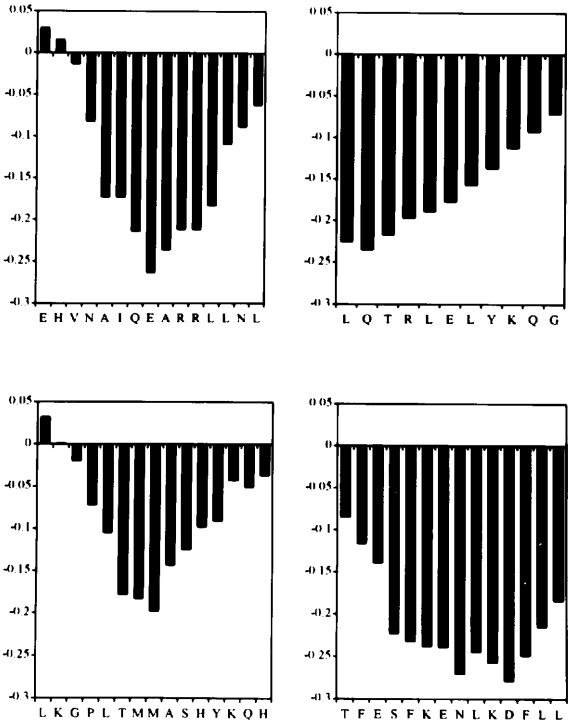

Figure 11 Deviations from the random coil position of the C^{α} resonances according to the method of Pastore and Saudek [23]. Clusters of five residues.

lower in the case of GM–CSF(55–65), possibly because of the reduced length of this peptide compared with the other ones. Another reason for this result could be the lack of inter-helical forces that stabilize the ordered conformation. In fact, from the crystal structure of GM–CSF it appears that only two residues of this short helix are accessible to the solvent, suggesting that contacts with other helices have a crucial stabilizing effect. When these interactions are not available, as in the isolated fragment, the helix stability is markedly decreased.

The importance of stabilizing inter-helical forces is demonstrated by the behaviour of GM–CSF(14–28) which undergoes a coil–helix conformational transition in aqueous solution induced by neutralization of the His residue at position 15. This peptide forms the most amphipathic helix among the four peptides under study (Figure 12). The helical stretch 17–27 has the highest mean hydrophobic moment of the entire hGM–CSF sequence and can be classified as a 'surface seeking sequence' [24]. The His^{15} residue is located in the middle of the hydrophobic portion of the helix cylinder and its neutralization is likely to favour inter-helical interactions through hydrophobic forces. This interpretation is supported by the concentration-dependence of the conformational

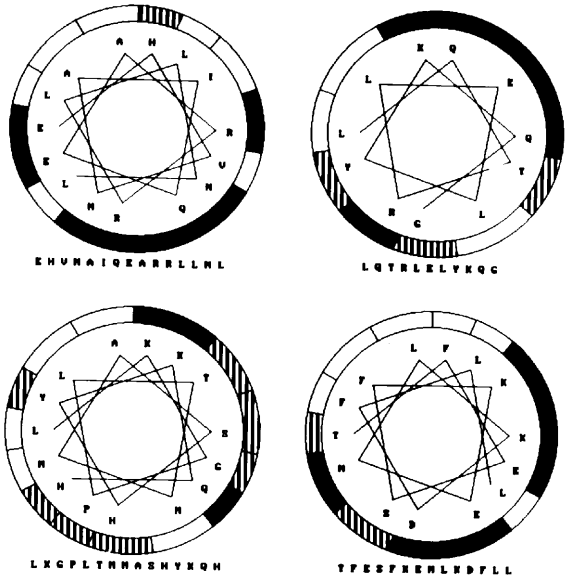

Figure 12 Shiffer-Edmunson projections of the α-helices formed by the four peptides.

change, common to many peptides forming amphipathic helices [25] and is in line with the inaccessibility to the solvent of the hydrophobic surface of helix A in the native protein [8]. The peptide GM–CSF(73–87), in spite of the presence of two His residues at positions 83 and 87, does not behave as helix A. This result can be explained with the much reduced mean hydrophobic moment of helix C.

The amounts of α-helix detected by NMR are in all cases much higher than those estimated by CD. This result is rather expected, given the length of the peptides under study and the solvent environment in which they were examined. From both these factors in fact, a high degree of flexibility in the peptide secondary structure can be anticipated. The indications from the two techniques confirm this prediction. Circular dichroism reflects an instantaneous average over all the molecules and gives an accurate indication of the relative amounts of the various conformers present. On the other hand, an NOE can be detected even if that specific short distance is present in a small percentage of the conformers, because of the inverse sixth power dependence of intensity upon distance. This means that, if the molecule is fluctuating between two limiting structures, NOEs can be found for both conformers present. This is indeed the case for all four peptides in this work, which show sequential αN cross-peaks as well as medium-range ones. Perhaps the secondary shifts of the C^{α} proton resonsances could provide a more quantitative evaluation of the

helical content of each amino acid residue, since this dependence should be linear. Nevertheless, the limited absolute value of the shifts and possibly local effects prevented us from reaching any firm conclusion.

Experiments are in progress to ascertain if the four synthetic peptides described in the present paper possess any biological activity. Although they show a tendency to fold into the native helix conformation they are not likely to be active as such. In fact, the minimal structure required for biological activity must include more than one helix. In native GM–CSF, helix A is close to helices C and D, and the interaction with the receptor α subunit seems to involve helix D and the C-terminal portion of helix A, while the N-terminal portion of helices A and C interact with the β subunit [13]. Having established that the four segments investigated here are capable of independent folding, our work will focus on synthetic segments comprising more helices.

Acknowledgements

This work was carried out with the financial support of Consiglio Nazionale delle Richerche (CNR) of Italy. The authors are indebted to Dr M. Hamdan of Glaxo-Wellcome Research Laboratories in Verona (Italy) for the mass spectrometry analysis.

REFERENCES

1. A. W. Burgess, J. Camakaris and D. Metcalf (1977). Purification and properties of colony-stimulating factor from mouse lung-conditioned medium. *J. Biol. Chem. 252*, 1998–2003.
2. M. Tomonaga, D. W. Golde and J. C. Gasson (1986). Biosynthetic (recombinant) human granulocyte-macrophage colony-stimulating factor: Effect on normal bone marrow and leukemia cell lines. *Blood 67*, 31–36.
3. D. Metcalf, C. G. Begley, G. R. Johnson, N. A. Nicola, M. A. Vadas, A. F. Lopez, D. J. Williamson, G. G. Wong, S. C. Clark and E. A. Wang (1986). Biologic properties *in vitro* of a recombinant human granulocyte-macrophage colony-stimulating factor. *Blood 67*, 37–45.
4. S. Vadhan-Raj, M. Keating, A. LeMaistre, W. N. Hittelman, K. McCredie, J. M. Trujillo, H. E. Broxmejer, C. Henney and J. U. Gutterman (1987). Effects of recombinant human granulocyte-macrophage colony-stimulating factor in patients with myelodysplastic syndromes. *New Engl. J. Med. 317*, 1545–1552.
5. J. E. Groopman, R. T. Mitsuyasu, M. J. DeLeo, D. H. Oette and D. W. Golde (1987). Effect of recombinant human granulocyte-macrophage colony-stimulating factor on myelopoiesis in the acquired immunodeficiency syndrome. *New Engl. J. Med. 317*, 593–598.
6. G. C. Baldwin, J. C. Gasson, S. G. Quan, J. Fleischmann, R. Weisbart, D. H. Oette, R. T. Mitsuyasu and D. W. Golde (1988). Granulocyte-macrophage colony-stimulating factor enhances neutrophil function in acquired immunodeficiency syndrome patients. *Proc. Natl Acad. Sci. USA 85*, 2763–2766.
7. S. J. Brandt, W. P. Peters, S. K. Atwater, J. Kurtzberg, M. J. Borowitz, R. B. Jones, E. J. Shpall, R. C. Bast, C. J. Gilbert and D. H. Oette (1988). Effect of recombinant human granulocyte-macrophage colony-stimulating factor on hematopoietic reconstitution after high-dose chemotherapy and autologous bone marrow transplantation. *New Engl. J. Med. 318*, 869–876.
8. K. Diederichs, T. Boone and P. A. Karplus (1991). Novel fold and putative receptor binding site of granulocyte-macrophage colony-stimulating factor. *Science 254*, 1779–1782.
9. M. R. Walter, W. J. Cook, S. E. Ealick, T. L. Nagabhushan, P. P. Trotta and C. E. Bugg (1992). Three-dimensional structure of recombinant human granulocyte-macrophage colony-stimulating factor. *J. Mol. Biol. 224*, 1075–1085.
10. K. Kaushansky and P. A. Karplus (1993). Hematopoietic growth factors: Understanding functional diversity in structural terms. *Blood 82*, 3229–3240.
11. D. P. Gearing, J. A. King, N. M. Gough and N. A. Nicola (1989). Expression cloning of a receptor for human granulocyte-macrophage colony-stimulating factor. *EMBO J. 8*,, 3667–3676.
12. K. Hayashida, T. Kitamura, D. M. Gorman, K. Arai, T. Yokota and A. Miyajima (1990). Molecular cloning of a second subunit of the receptor for human granulocyte-macrophage colony-stimulating factor (GM–CSF): Reconstitution of a high affinity GM–CSF receptor. *Proc. Natl Acad. Sci. USA 87*, 9655–9659.
13. G. J. Goodall, C. J. Bagley, M. A. Vadas and A. F. Lopez (1993). A model for the interaction of the GM–CSF, IL-3 and IL-5 receptors with their ligands. *Growth Factors 8*, 87–97.
14. N. Greenfield and G. D. Fasman (1969). Computed circular dichroism spectra for the evaluation of protein conformation. *Biochemistry 8*, 4108–4116.
15. S. Pegoraro, P. Rovero, S. Viganò, R. Revoltella, S. Fiori, S. Mammi and E. Peggion. in: *Peptides 1994*, Proceedings of the 23rd European Peptide Symposium, H. L. S. Maia, Ed., p. 533–534, ESCOM, Leiden 1995.
16. J. B. Siegel, W. E. Steinmetz and G. L. Long (1980). A computer-assisted model for estimating protein secondary structure from circular dichroic spectra: Comparison of animal lactate dehydrogenases. *Anal. Biochem. 104*. 160–167.
17. G. Drobny, A. Pines, S. Sinton, D. Weitekamp and D.

Wemmer (1979). Fourier transform multiple quantum nuclear magnetic resonance. *Symp. Faraday Soc. 13*, 49.
18. G. Bodenhausen, R. L. Vold and R. R. Vold (1980). Multiple quantum spin-echo spectroscopy. *J. Magn. Reson. 37*, 93–106.
19. M. Rance, O. W. Sørensen, G. Bodenhausen, G. Wagner, R. R. Ernst and K. Wüthrich (1983). Improved spectral resolution in COSY proton NMR spectra of proteins via double quantum filtering. *Biochem. Biophys. Res. Commun. 117*, 479–485.
20. A. E. Derome and M. P. Williamson (1990). Rapid-pulsing artifacts in double-quantum-filtered COSY. *J. Magn. Reson. 88*, 177–185.
21. C. Griesinger, G. Otting, K. Wüthrich and R. R. Ernst (1988). Clean TOCSY for ^{1}H spin system identification in macromolecules. *J. Am. Chem. Soc. 110*, 7870–7872.
22. S. Macura and R. R. Ernst (1984). Elucidation of cross-relaxation in liquids by two-dimensional N.M.R. spectroscopy. *Mol. Phys. 41*, 95–117.
23. A. Pastore and V. Saudek (1990). The relationship between chemical shift and secondary structure in proteins. *J. Magn. Reson. 90*, 165–176.
24. D. Eisenberg, E. Schwarz, M. Komaromy and R. Wall (1984). Analysis of membrane and surface protein sequences with the hydrophobic moment plot. *J. Mol. Biol. 179*, 125–142.
25. J. P. Segrest, H. DeLoof, J. G. Dohlman, C. G. Brouillette and G. M. Anantharamaiah (1990). Amphipathic helix motif: Classes and properties. *Proteins 8*, 103–117.

